Experimental analysis of cellular detonations: a discussion on regularity and three-dimensional patterns

V. Monnier, V. Rodriguez, P. Vidal and R. Zitoun
Institut Pprime, UPR 3346, ENSMA, BP 40109, 86961 Futuroscope-Chasseneuil, France

1 Introduction

The cellular structure of detonation fronts in gases has been a long-time subject of a large number of experimental and numerical investigations. Its understanding is considered necessary for sizing safe industrial devices and advanced propulsion systems [1], and for its fundamental interest as a dramatic illustration of non-linear instabilities in compressible reactive fluid dynamics [2].

Its description relies on lengths such as the cell mean width [3] or the hydrodynamic thickness [4], and on the low or high regularity of the diamond-shape patterns left by the detonation front sweeping soot foils positioned at the tube walls [4–6]. Measurements and calculations have been carried out for many reactive mixtures, depending on their equivalence ratio, their initial pressure, temperature and composition, their confinements such as straight or curved tubes and channels, and their dynamical behaviors such as transmissions from tubes to large volumes. The chapters by Higgins, Ng and Zhang, Vasil'ev, and Desbordes and Presles in [7] present extensive reviews.

Its numerical modelling requires capturing a large range of orders of magnitude, from the reaction zone length to the characteristic size of the system. The computing costs are thus often decreased using reductions of the size of the chemical-kinetics scheme, the problem dimension to 2D geometries, or the numerical resolution for 3D geometries. These simplifications imply adjustments of parameters that make it difficult to ensure the capture or the identification of the relevant physics.

Only a limited number of experimental studies has addressed the 3D features of the cellular structure, for example, based on head-on visualizations of cellular detonation fronts [8–11]. Presles et al. [11] thus suggested to further investigate the effects of the confinement geometry. Our work is an experimental analysis of the effect of the cross-section shape of detonation tubes on the cellular structure of the $2\,H_2$ + O_2 + 2 Ar mixture, based on head-on and longitudinal recordings on soot-coated foils.

2 Methodology

We carried out a series of recordings in tubes with the same area - to within ± 4 % - but different shapes of their cross sections, namely round (R), equilateral triangular (T) and square (Q). We also used round and square tubes with larger cross sections (R' and Q' resp.). The dimensions of the tubes are given in table 1.

We chose the diluted stoichiometric reactive mixture $2\,H_2 + O_2 + 2\,Ar$ because its regular cellular pattern in Q tubes at low-enough initial pressures [12] is a convenient reference for comparison with the patterns in the R and T tubes . The mixture was prepared in a separate tank using the partial-pressure method, and then injected at the desired initial pressure p_0 after vacuuming the tubes. The initial temperature was 294 ± 3 K for all experiments.

A spark plug or an exploding wire was used for ignition ; Shchelkin spirals then ensured the transition to detonation on a very short distance, typically 1 m. The 1-m long T tube was inserted at the end opposite to ignition of the 10-m long R' tube so that the detonation be steady before entering the T tube.

Longitudinal and head-on recordings of the cellular structure were obtained using soot-coated foils positioned at the tube ends opposite to ignition. The longitudinal foils were shaped as half cylinders for the R tubes and plates for the Q tubes, and positioned at the tube walls. They were 50-cm long and 0.15-mm thick for the R and Q tubes. The three inner faces of the T-tube were individually coated with soot and then assembled with sharp equal inner angles.

Three Kistler 603B pressure transducers coupled with Kistler 5018A electrostatic charge amplifiers were positioned on each tube before the soot-foil section. The triggering of the transducers was used to obtain the average velocity of the detonation wave and check its steadiness in the soot-foil section. The steadiness was also checked from the longitudinal recordings showing constant cell lengths from the beginning to the end of each soot foil, except for a few centimeters of adjustment at the T-tube entry. Soot foils were also positionned at the middle of the Q and R tubes to verify the independence of the cells of the position of the recordings.

Table 1: Inner dimensions of the tubes. R,R': round, T: equilateral triangle, Q,Q': square

Tube	Cross-section area (cm^2)	Diameter or side length (mm)	Length (m)
R	16.6	46	6
T	16.1	61	1
Q	16.0	40	6
R'	70.8	95	10
Q'	25.0	50	6

3 Results

Figure 1 shows typical head-on and longitudinal soot recordings for the two initial pressures $p_0 = 15$ and 22.5 kPa.

At lower initial pressures, up to $p_0 = 17.5$ kPa, the head-on soot recordings in the Q tube reaffirm the long-time identified regular arrangement of square and rectangular patterns [8] whose distributions depend on the instant of the detonation impact. However, their arrangements in the T and R tubes are irregular, and repeated experiments show, statistically, no dependency on the instant of impact. Although their counting is difficult, more cells appear to be contained in the Q tube than in the others, and in the T tube than in the R tube - that is, given the same cross-section area - for the same p_0.

In the intermediate range $p_0 = 17.5$ - 70.0 kPa, the head-on soot recordings in the Q tube show the stochastic emergence of domains with distorted rectangular and square patterns whose number and extent increase with increasing p_0. The arrangements in the T and R tubes are irregular. Regardless of the tube, the cells are smaller than at lower p_0, and the larger ones are observed in the R tube.

At larger p_0, from about 70.0 kPa, the head-on soot recordings in the Q tube (shown in Figure 3 for layout convenience) show irregular patterns similar to those in the T and R tubes, that is, the head-on patterns at large p_0 become irregular and independent of the cross-section shape, whose effect on the cell shape thus decreases with increasing p_0.

The longitudinal soot recordings point to three observations. The first is the paradoxical result that the longitudinal patterns are systematically regular even in the cases where the head-on patterns are not, regardless of the tube. This suggests that characterizing detonation cells cannot rely only on reduced 2D information from the tracks left on longitudinal recordings and also raises questions on the causes of cell regularity. The cellular dynamics at the walls of a tube thus appears not representative of that on the whole detonation front. The second is that there are no slapping waves in the T and R tubes regardless of p_0, and in the Q tube at large enough p_0. This is coherent with the increase of cell irregularity with increasing p_0 shown by the head-on recordings. The third is that the cells are slimmer in the Q tube than in the T and R tubes, i.e. their width-to-length aspect ratio is smaller. One interpretation is that mode-locking in the Q tube (the number of cells across the tube is an integer [6]) modifies the ratio of the transverse and longitudinal wave velocities, compared to that in a R or a T tube.

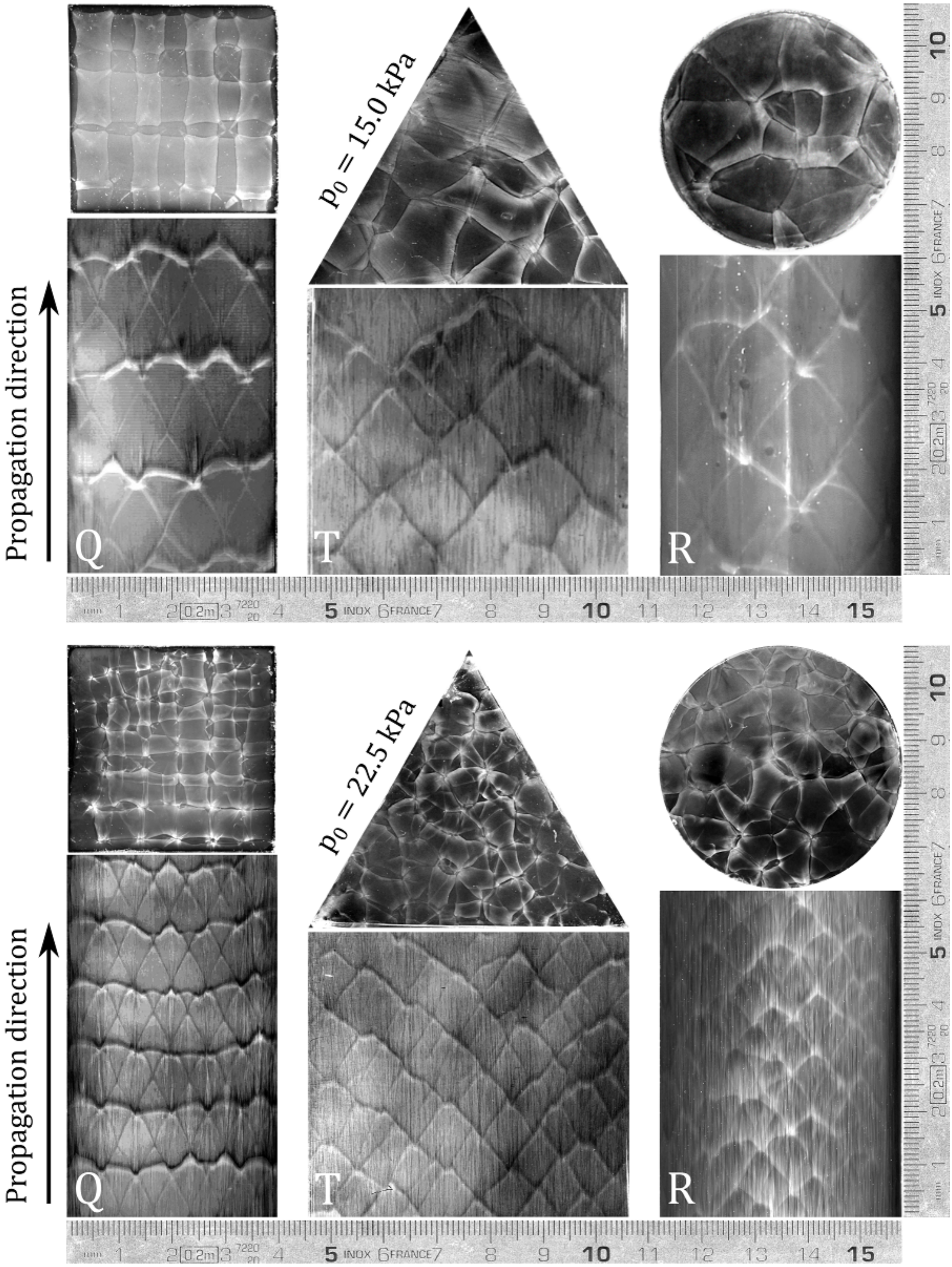

Figure 1: Head-on (upper) and longitudinal soot recordings at $p_0 = 15.0$ and 22.5 kPa in round (R), triangular (T) and square (Q) tubes with cross-section area 16 cm^2 (reactive mixture: $2\,H_2 + O_2 + 2\,Ar$).

The grey levels on the head-on recordings in Figure 1 can be used to infer the propagation direction of the transverse waves, precisely from the lighter to the darker domains. Indeed, the latter represent the soot particles before the transverse waves sweep them. Figure 2 shows a schematic for the Q tube, where x and y denote the two transverse directions, and z the longitudinal one. The joint analyses of the longitudinal and head-on soot recordings in the Q tube at low enough p_0 thus reveal a continuous modulation of the phase shift - the distance φ between the longitudinal positions of the reflections in the x and y directions of the orthogonal transverse waves - as the detonation propagates (Fig. 2). The out-of-phase modes ($\varphi \neq 0$, the x and y transverse waves reflect at different positions on their respective walls) are generally observed. Figure 2-top shows the particular out-of-phase mode for which φ has its maximum value φ_{max} equal to half a cell length, i.e. the phase-opposition mode. The head-on capture of the in-phase mode ($\varphi = 0$, the x and y transverse waves reflect simultaneously, at the same position z) is thus a fortuitous event (Fig. 2-bottom). One interpretation is that the expanding flow behind the self-sustained detonation front is subjected to long-wavelength and low-amplitude instabilities - compared to the cell dynamics - that distort the average front, so its surface is warped, hence the evolutive-mode dynamics. These instabilities might result from the ignition and the system itself, such as the non-symmetric wave coming out from the Shchelkin spiral and small defects at the tube walls.

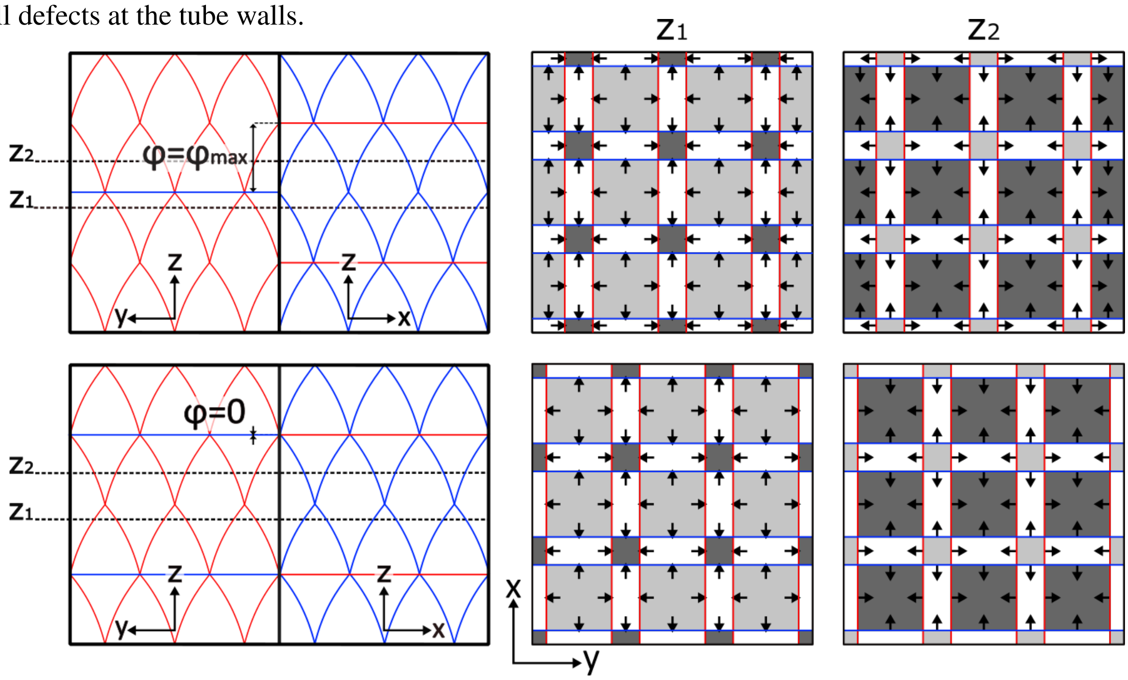

Figure 2: Schematics of the in-phase mode (top, $\varphi = 0$) and the out-of-phase mode with phase opposition (bottom, $\varphi = \varphi_{max}$)

The phase shift used above for multicellular detonation fronts generalizes that introduced in former experimental analyses for the particular case of the marginal detonation with one cell per tube. Hanana et al. [8] and Williams et al. [14] addressed the cases $\varphi = 0$ and φ_{max}, respectively. Tsuboi et al. [15], Wang et al. [13] and more recently Taileb et al. [16] presented simulations of these marginal cases based on the Euler inviscid fluid model. The continuous modulations described in our work actually make the phase shift often difficult to measure with a practical accuracy, and thus a tool restricted to an ideal cellular detonation front, that is, neither tilted, curved, nor warped. These observations are specific to the cell dynamics in a Q tube. The increase of the acquisition frequencies of high-speed cameras should soon allow obtaining directly head-on cellular kinematics regardless of the tube.

Figure 3 shows the cell mean width λ measured on the longitudinal soot recordings as a function of p_0 for each cross-section shapes and areas. The values of λ are averages over about 50 measurements along each

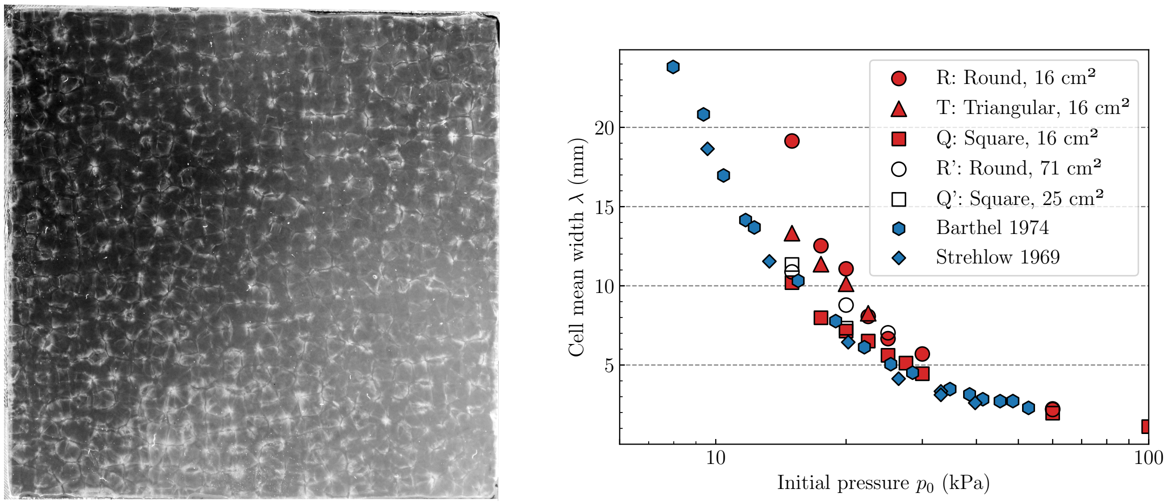

Figure 3: Left: head-on soot recording at $p_0 = 70.0$ kPa in the Q tube. Right: cell mean width measured at walls as function of the initial pressure. Measurement uncertainty is about the same as the marker height.

recording ; the resulting uncertainty is approximately the same as the height of the coordinate markers. The plot indicates that the effect of the cross section on λ decreases with increasing p_0: the cell widths and their relative differences at constant p_0 from one cross-section to another are decreasing functions of p_0, the larger differences are obtained with the Q and the R tubes, and these differences can be as large as $\sim 100\%$ at the lower value $p_0 = 15$ kPa. The λ values for the T tube are always comprised between those of the Q and R tubes. However, whereas the difference of λ between the Q and R tubes progressively increases with decreasing p_0, that between the T and R tubes appears more abrupt. This graph thus substantiates the questioning above on the representativeness of λ and thus on how to parameterize the cellular structure. Nevertheless, the classical empirical relation $\lambda \propto p_0^{\alpha}$, $-1.3 < \alpha < -1.1$, is satisfied at larger p_0, e.g., [9].

4 Discussion and conclusion

The results above suggest that the cellular dynamics obtained from longitudinal (wall) recordings cannot represent alone the cellular structure on the whole detonation front: for the considered stable mixture, they always show regular patterns even in the conditions for which the head-on recordings show irregular patterns. The development of an irregular head-on structure in a square tube with decreasing cell size relative to the tube width may also indicate that head-on regularity essentially results from acoustic forcing. An irregular structure may thus be most representative as the propagation conditions approaches those of the average CJ regime.

They also indicate that this boundary effect at walls and the initial conditions of ignition might have a long-range influence on a 3D regular structure in square tubes because of the continuous variation of the phase shift as the detonation propagates. This suggests two modelling hypotheses. The first is to perform inviscid-fluid simulations on much longer times and lengths than those accepted so far so that long-wavelength and low-amplitude instabilities can possibly emerge. The second is to include small influences of turbulence and viscosity phenomena, which implies numerical simulations based on the Navier-Stokes equations.

The acoustic influence on cell size and regularity is a decreasing function of the initial pressure that depends on the cross-section shape. For the considered mixture, the cell patterns are the more regular in the square tubes. all head-on patterns appear irregular if they are independent of the shape and the area of the cross section. This requires to be close enough to the 1D-CJ regime, away from the propagation limits, with small cell size-to-tube width ratio, but these conditions are difficult to anticipate.

The cell regularity and mean width (or any single length, such as a hydrodynamic length), as usually defined from two-dimensional measurements at walls, may not always be relevant parameters for scaling dynamical behaviours of DDT processes and cellular detonations in gases, e.g., [17, 18]. Indeed, many involve at least an acoustic interplay with chemical kinetics and show cells larger than for the CJ propagation. Therefore, the detonation cellular structure should be described as a three-dimensional phenomenon. The quantitative capture of this complex three-dimensional interplay of chemical kinetics and transverse reflections of shocks at walls requires high-resolution numerical simulations based on the inviscid-fluid (Euler) equations and a detailed scheme of chemical kinetics. Nevertheless, modelling could draw advantage from more advanced conceptual tools than a single length, for example a Voronoi tesselation supplemented with a physical criterion for point sources representing the explosions locii from transverse interactions. Graph theory can also be used to demonstrate that a head-on distribution of hexagons is equivalent to a head-on distribution of a large number of cells [19].

References

[1] Shepherd J.E., Kasahara J. (2017). Analytical Models for the Thrust of a Rotating Detonation Engine. Technical Report FM2017.001, Graduate Aeronautical Laboratories, California Institute of Technology 10.7907/DNVT-PY80

[2] Clavin P., Searby G. (2016). Combustion Waves and Fronts in Flows: Flames, Shocks, Detonations, Ablation Fronts and Explosion of Stars. Cambridge University Press. 10.1017/CBO9781316162453

[3] Vasil'ev A. A. (2006). Cell Size as the Main Geometric Parameter of a Multifront Detonation Wave, J. Propuls. Power, 22:6, 1245-1260 10.2514/1.20348

[4] Lee J.H.S., Radulescu M.I. (2005). On the Hydrodynamic Thickness of Cellular Detonations. Comb. Expl. Shock Wave, 41, 745–765. 10.1007/s10573-005-0084-1

[5] Jackson S.I., Short M. (2013). The influence of the cellular instability on lead shock evolution in weakly unstable detonation, Combust. Flame, 160:10, 2260-2274. 10.1016/j.combustflame.2013.04.028

[6] Sharpe G.J., Quirk J.J. (2008). Nonlinear cellular dynamics of the idealized detonation model: Regular cells, Combust. Theor. Model., 12:1, 1-21, 10.1080/13647830701335749

[7] Shock Waves Science and Technology Library, vol.6, Detonation Dynamics, Springer, Berlin, Heidelberg. 2012, 10.1007/978-3-642-22967-1

[8] Hanana M., Lefebvre M.H., Van Tiggelen P.J. (1998). On Rectangular and Diagonal Three-Dimensional Structures of Detonation Waves, Int. Coll. on Advances in Experimentation & Computation of Detonations

[9] Shchelkin K.I., Troshin Ya.K. (1965). Gasdynamics of combustion. National Aeronautics and Space Administration, Tech. Translation, 231

[10] Takai R., Yoneda K., Hikita. T. (1975). Study of detonation wave structure, Proc. Combust. Inst., 15:1, 69-78, 10.1007/10.1016/S0082-0784(75)80285-2

[11] Presles H.N., Desbordes D., Bauer P. (1987). An optical method for the study of the detonation front structure in gaseous explosive mixtures, Combust. Flame, 70, 207-213 10.1016/0010-2180(87)90079-4

[12] Lee J.H.S. (2008). Unstable detonations: Experimental observations. *In* The Detonation Phenomenon, 147-203. Cambridge University Press. 10.1017/CBO9780511754708.007

[13] Wang C., Shu C.W., Han W., Ning J. (2013). High resolution WENO simulation of 3D detonation waves, Combust. Flame; 160:447-62. 10.1016/j.comb. flame.2012.10.002

[14] Williams D. N., Bauwens L. (1996). Detailed structure and propagation of three-dimensional detonations, Twenty-Sixth Symposium (Int.) on Combustion/The Combustion Institute, 2991–2998 10.1016/S0082-0784(96)80142-1

[15] Tsuboi N., Katoh S., Hayashi A. (2002). Three-dimensional numerical simulation for hydrogen/air detonation: Rectangular and diagonal structures, Proc. Combust. Inst., 29, 2783-2788 10.1016/S1540-7489(02)80339-X

[16] Taileb S., Reynaud M., Chinnayya A. (2018). Numerical study of 3D gaseous detonations in a square channel, Aerotec. Missili Spaz. 97, 96–102. 10.1007/BF03405804

[17] Rodriguez V., Monnier V., Vidal P., Zitoun R. (2021). On the possibility of non-dimensionalizing DDT limits and distances, to be presented as an oral presentation at the 28^{th} ICDERS, Napoli (2022), hal-03424349

[18] Rodriguez V., Monnier V., Vidal P., Zitoun R. (2022). Towards non-dimensionalized distances and limits for transition of deflagration to detonation (under revision), Shock Waves, hal-03424392

[19] Monnier V., Rodriguez V., Vidal P., Zitoun R. (2022). An analysis of three-dimensional patterns of experimental detonation cells (under revision), Combust. Flame, hal-03632291